

MASTER OF SCIENCE THESIS

Geometric Control of a Quadrotor with a Suspended Load

Subtitle

N.N. Vo

June 13, 2017



Geometric Control of a Quadrotor with a Suspended Load

Subtitle

MASTER OF SCIENCE THESIS

For obtaining the degree of Master of Science in Mechanical
Engineering at Delft University of Technology

N.N. Vo

June 13, 2017

The work in Master of Science Thesis was supported by Alten. Their cooperation is hereby gratefully acknowledged.



Delft University of Technology

Copyright © Delft Center for Systems and Control
All rights reserved.

DELFT UNIVERSITY OF TECHNOLOGY
DELFT CENTER FOR SYSTEMS AND CONTROL

The undersigned hereby certify that they have read and recommend to the Faculty of Mechanical, Maritime and Materials Engineering for acceptance a thesis entitled “**Geometric Control of a Quadrotor with a Suspended Load**” by **N.N. Vo** in partial fulfillment of the requirements for the degree of **Master of Science**.

Dated: June 13, 2017

Supervisor:

dr.ir. T. Keviczky

Readers:

ir. B. van Vliet

Abstract

A Quadrotor is a type of Unmanned Aerial Vehicle that has received an increasing amount of attention recently with many applications including search and rescue, surveillance, supply of food and medicines as disaster relief and object manipulation in construction and transportation.

An interesting control problem is the Load Position Tracking of a cable suspended load. The system is highly nonlinear and under-actuated. The load cannot be actuated directly and has a natural swing at the end of each Quadrotor movement. A Nonlinear Geometric Control approach allows differential geometric techniques to be applied to systems control, which can be defined on a smooth nonlinear configuration space. This creates a coordinate-free dynamic model, while avoiding the problem of singularities on local charts.

Intro about GC.. Reasons to consider GC..

Where simple linear control methods are restricted to small angle movements, nonlinear control methods allow more aggressive and faster movements. The goal of the project is to investigate the effects on load position tracking performance when the system is modeled and controlled via a Nonlinear Geometric Control approach.

The Quadrotor-Load system is modeled in a compact and coordinate-free fashion which allows the inherent geometric properties of the system to be controlled.

The main goal of this thesis is to research the effects on a cable-suspended load transportation using quadrotors, by involving complex or aggressive maneuvering through implementation of Non-Linear Geometric Control. Where linear control methods are restricted to small angle movement, non-linear control methods allow more aggressive movements.

Furthermore, the studied control techniques are explained and their advantages are addressed. Several trajectory generation approaches and the related optimization techniques are studied. Their applications, with different purposes such as obstacle avoidance, time-optimal and swing-free trajectory planning are explained. The survey is concluded with a discussion

about finding a suitable *****

Define suitable

control design to achieve the quadrotor-assisted task involving manipulation of a cable-suspended load.

Acknowledgements

I would like to thank my supervisors dr.ir. T. Keviczky from DCSC and ir. B. van Vliet from Alten Nederland B.V. for their assistance during the writing of this thesis. I would also like to thank all other Alten- and student colleagues for their time and advice whenever it was needed.

Delft, University of Technology
June 13, 2017

N.N. Vo

Table of Contents

Abstract	v
Acknowledgements	vii
1 Introduction	1
1-1 Aim and Motivation	1
1-2 Organization of the Report	3
2 Dynamic Model	5
2-1 Modeling Assumptions	6
2-2 Geometric Mechanics	7
2-3 Quadrotor-Load Model	11
2-4 Classical Modeling	12
2-5 Stability Analysis	14
2-6 Summary	14
3 Geometric Control Design	17
3-1 Backstepping Control	17
3-2 Configuration Errors	18
3-3 Quadrotor Attitude Tracking	20
3-4 Load Attitude Tracking	20
3-5 Load Position Tracking	21
3-6 Parameter- and State Estimation	21
3-7 Summary	21

4	Experiments and Results	23
4-1	Setup	23
4-1-1	Command Filtering	24
4-2	Experiments	25
4-2-1	Performance Criteria	25
4-2-2	Case A	26
4-2-3	Case B	26
4-2-4	Case C	26
4-3	Results	26
4-3-1	Case A	26
4-3-2	Case B	26
4-3-3	Case C	26
4-4	Conclusion	26
5	Conclusions and Future Work	27
5-1	Summary and Conclusions	27
5-2	Recommendations for Future Work	27
5-2-1	Modeling Constraints	27
5-2-2	Hybrid Modeling	27
5-2-3	Trajectory Generation	28
	Minimum Snap Trajectory Generation	28
A	Appendix	29
A-1	Derivation of Equations of motion	29
A-1-1	Load Dynamics	29
A-2	Derivation of LQR controller	29
A-2-1	Modeling	29
A-2-2	Controller	30
A-3	MATLAB code	31
A-3-1	A MATLAB Listing	31
	Bibliography	35
A-4	Figures	37
	Acronyms	38

List of Figures

2-1	Quadrotor model representation	6
2-2	Quadrotor with Load model representation	6
2-3	A manifold locally resembles a Euclidean space	9
2-4	9
2-5	Configuration Space of a 2-link arm	10
2-6	Quadrotor-Load model representation	11
2-7	Quadrotor-Load model representation	13
2-8	14
3-1	Backstepping Control representation of the QR	18
3-2	Backstepping Control representation of the QR-Load system	18
3-3	20
3-4	21
3-5	21
4-1	LQR control design	24
4-2	Representation of the command filter	25
4-3	Cases of which the performance could be evaluated	26

List of Tables

2-1	Modeling assumptions Quadrotor model	7
2-2	Modeling assumptions Quadrotor+Load model	8

Chapter 1

Introduction

A Quadrotor (QR) is a type of Unmanned Aerial Vehicle (UAV) that has received an increasing amount of attention recently with many applications being actively investigated. Possible applications include search and rescue, surveillance, reliable supply of food and medicines as disaster relief and object manipulation in construction and transportation. It has already proven itself useful for many tasks like multi-agent missions, mapping, explorations, transportation and entertainment such as acrobatic performances.

Considering a multi-agent task, one can think of multiple QRs assisting in the transportation of a common load. This cooperation can be executed in many ways, but this literature focuses on QRs with a cable-suspended load in motion. The suspended object naturally continues to swing at the end of every movement. In case a residual motion can result in damage or in order to avoid obstacles and path following, an accurate positioning is required. Reducing the oscillation, or controlling the position of the suspended load might be necessary, but is challenging in the fact that this cable-suspended system is under-actuated.

In this chapter, firstly the aim and motivation for this research are given. Next, the contributions given by this research are explained. And finally, the organization of the report is presented.

Suggestion place under motivation of research inspiration, this forms a nice bridge

1-1 Aim and Motivation

The inspiration for this research is build upon the idea of creating multiple autonomous QR system for a cooperative towing task. The advantage of using multiple robots for object manipulation is the possibility to reduce complexity of the individual robot, decrease cost over traditional robotic systems and high reliability. One can think of examples in nature, where individuals coordinate, cooperate and collaborate to perform tasks that they individually can not accomplish. Redundancy makes development of fail safe control methods possible and can extend the capabilities of a single robot.

The aim is to control the position of a suspended load using a QR. In this research a single QR is considered for the transportation of a cable suspended load, which will exert forces and

torques on the QR. This is challenging control problem in the fact that the QR-Load system is under-actuated and oscillations of the load occur at the end of every movement. Possible objectives are minimizing the oscillations of the load during and after motion, or minimizing the time to bring the load to a desired position, using active control techniques.

Former work on QR attitude- and position control often rely on linear control methods such as PID controller[?], MPC [1] and LQR control [?]. The dynamics are linearized around an equilibrium point, describing the system dynamics by a set of linear differential equations.

The control of a QR-Load system is a more specific case, and therefore found less in literature. An optimal control strategy is able to minimize the swing of the load. Former work include MPC [2] and LQR[?] control approaches.

The reason that linear control near an equilibrium state is commonly applied is partly to avoid difficulties that come with modeling and controlling the non-linearities of the system. However, this limits the system to small angle movements, as the optimization will not allow large angles due to the linearization.

Non-linear control systems are often governed by nonlinear differential equations. Nonlinear MPC is a variant of MPC which uses a nonlinear dynamical system to predict the required inputs. High computational cost. While these problems are convex in linear MPC, in nonlinear MPC they are not convex anymore. This poses challenges for both Nonlinear MPC stability theory and numerical solution.

Geometric Control, a nonlinear model based control technique based on a modeling approach involving differential geometry, is found less common in literature. However, the concepts of differential geometry result in a globally defined coordinate-free dynamical model, while preventing issues regarding singularities, and enabling the design of controllers that offer almost-global convergence properties.

Dynamics and optimal control problems for rigid bodies are studied in [3], incorporating their geometric features. The focus lies on obtaining geometric properties of the dynamics of rigid bodies, how their configuration can be described and how these geometric properties are utilized in control system analysis and design.

A nonlinear geometric PID controller control for a QR is studied in [4]

Controllers for a QR-Load system are proposed in [5, 6].

This motivates to investigate the possibilities and limitations of a non-linear Geometric Control design, when it is compared to a linear control strategy.

A controller is designed a priori to guarantee global asymptotic stability. Unlike a MPC approach, the

What can we learn and conclude from different performance comparisons

What is its value compared against linear control

Could it be interesting for a real-time on-board controller Considering the computational power of an on-board processor is limited computational effort vs what?

Geometric Mechanics and Control is used to understand the structure of the equations of motion of a system in order to allow its analysis and design. The system evolves on a nonlinear manifold and the controllers are designed on this same manifold.

Different aspects involving the modeling and control for the QR-Load system must be investigated, for it can be expected that the non-linearity will have a great influence in the representation of the dynamics and the stability, accuracy and type of control design.

System consists of two sub-systems Limited to subsystem where the tension of the cable is non-zero.

1-2 Organization of the Report

- Chapter 1
- Chapter 2
- Chapter 3
- Chapter 4
- Chapter 5
- Chapter ??

Chapter 2

Dynamic Model

The dynamics of the QR-Load system are described by the laws of kinematics and the application of Newton's laws or Lagrangian mechanics. Opposed to the classical modeling techniques, it is also possible to describe the system's configuration space as a differentiable manifold using the tools of differential geometry.

Considering the properties of the system, the QR is described as a rigid body with six degrees of freedom, driven by forces and moments. The motion of a rigid body can be described by a translation of the Center of Mass (CoM) and a rotation about the CoM. The derived mathematical model is represented by a set of dynamic equations commonly used for rigid body displacements.

To derive the equations of motions traditional modeling methods often parameterize the rotations in a local coordinate system. Euler angles are commonly used, however these coordinates might result in singularities. Furthermore, there are 24 sets of Euler angles, which can lead to ambiguity. In order to avoid these complexities, the dynamics of the QR-Load system can be globally expressed on the Special Orthogonal Group $SO(3)$, 2-sphere S^2 and Special Euclidean Group $SE(3)$. This leads to a compact notation of the equations of motion, making the large amount of trigonometric functions unnecessary, that Euler angles normally introduce.

An Introduction to Differentiable Manifolds is given by [7]

[8] [9]

Computational Geometric Mechanics and Control

Computation algorithms must be developed which preserve the geometric properties of a mechanical system.

Robust and careful numerical implementation of geometric control theory to complex engineering systems.

Provides nontrivial maneuvers that are globally valid on a nonlinear configuration manifold.

2-1 Modeling Assumptions

A mathematical model of the system needs to be derived in order to simulate and study the effects of Geometric Control. The following assumptions are applied to simplify the model.

The QR model representation is shown in Figure 2-1. Three Cartesian coordinate frames are defined:

- The body-fixed reference frame $\{\mathcal{B}\}$ (Body Frame)
with unit vectors $\{\mathbf{b}_1, \mathbf{b}_2, \mathbf{b}_3\}$ along the axes
- The ground-fixed reference frame $\{\mathcal{I}\}$ (Inertial Frame)
with unit vectors $\{\mathbf{e}_1, \mathbf{e}_2, \mathbf{e}_3\}$ along the axes
- The intermediary frame $\{\mathcal{C}\}$, ($\{\mathcal{I}\}$ rotated by the yaw angle ψ)
with unit vectors $\{\mathbf{c}_1, \mathbf{c}_2, \mathbf{c}_3\}$ along the axes



Figure 2-1: Quadrotor model representation



Figure 2-2: Quadrotor with Load model representation

The position of the body frame is described by a vector evolving on \mathbb{R}^3 , and is represented with respect to the inertial frame. The orientation, also called attitude, of the body frame with respect to the inertial frame evolves on a nonlinear space, for which several methods exist to describe this, such as *Euler Angles*, quaternions or rotation matrices.

The complex dynamics of the rotors and their interactions with drag and thrust forces are represented by a simplified model. The angular speed ω_i of rotor i , for $i = 1, \dots, 4$, generates a force F_i parallel to the direction of the rotor axis of rotor i , given by

$$F_i = \left(\frac{K_v K_\tau \sqrt{2\rho A}}{K_t} \omega_i \right)^2 = b\omega_i^2 \quad (2-1)$$

where K_v, K_t are constants related to the motor properties, ρ is the density of the surrounding air, A is the area swept out by the rotor, K_τ is a constant determined by the blade configuration and parameters, and b is the thrust factor.

The torque around the axis of rotor i , for $i = 1, \dots, 4$, generated due to drag is given by


$$M_i = \frac{1}{2} R \rho C_D A (\omega_i R)^2 = d \omega_i^2 \quad (2-2)$$

where R is the radius of the propeller, C_D is a dimensionless constant, and d is the drag constant.

For given desired total thrust f and total moment $M = [M_\phi \ M_\theta \ M_\psi]^T$, the required rotor speeds can be calculated by solving the following equation

$$\begin{bmatrix} f \\ M_\phi \\ M_\theta \\ M_\psi \end{bmatrix} = \begin{bmatrix} b & b & b & b \\ 0 & -Lb & 0 & Lb \\ Lb & 0 & -Lb & 0 \\ -d & d & -d & d \end{bmatrix} \begin{bmatrix} \omega_1^2 \\ \omega_2^2 \\ \omega_3^2 \\ \omega_4^2 \end{bmatrix} \quad (2-3)$$

where L is the cable length and M_ϕ, M_θ, M_ψ denote the moments around the x, y, z -axis in $\{\mathcal{B}\}$, resp.

Table 2-1 shows the most common assumptions that are used for modeling the QR, simplifying the complexity of the model. 

- The structure of the QR is rigid and symmetric.
Elastic deformations and shock (sudden accelerations) of the QR are ignored.
- The mass distribution of the QR is symmetrical in the x-y plane.
- The inertia matrix is time-invariant.
- Aerodynamic effects acting on the QR are neglected.
Blade flapping, Turbulence, Ground Effects.
- The air density around the QR is constant.
- The propellers are rigid \Rightarrow The thrust produced by rotor i is parallel to the axis of rotor i .
- Drag factor d and thrust factor b are approximated by a constant.
Thrust force F_i and moment M_i of each propeller is proportional to the square of the propeller speed.

Table 2-1: Modeling assumptions Quadrotor model

2-2 Geometric Mechanics



In this section an introduction is given about Geometric Mechanics, which is a modern description of the classical mechanics from the perspective of Differential Geometry, which is a discipline in mathematics that studies manifolds and their geometric properties, using the tools of calculus. Geometric Mechanics is used to model the QR-Load system, which is described in Section 2-3.

In Geometric Mechanics the configuration space of systems is a *group manifold* instead of a Euclidean space. The kinetic and potential energies are expressed in terms of this configuration space and their tangent spaces. It explores the geometric structure of a Lagrangian-


- The cable is modeled as a rigid and massless cable.
- The cable is connected to a friction-less joint at the origin of the body-fixed.
- The tension in the cable is considered to be non-zero.
This implies that the QR-Load subsystem, consisting of a separate QR and Load in free fall, is disregarded.
- Aerodynamic effects acting on the load are neglected.
reference frame.
- Assumption
Details Assumption 2

Table 2-2: Modeling assumptions Quadrotor+Load model

or Hamiltonian system through the concepts of vector calculus, linear algebra, differential geometry, and non-linear control theory. Geometric mechanics provides fundamental insights into the non-linear system mechanics and yields useful tools for dynamics and control theory.

 Mechanics studies the dynamics of physical bodies acting under forces and potential fields. In Lagrangian  mechanics, the trajectories are obtained by finding the paths that minimize the integral of a Lagrangian over time, called the action integral. Rigid body dynamics are characterized by Lagrangian/Hamiltonian dynamics. The dynamics of a Lagrangian system has unique geometric properties and these are exploited to obtain Euler-Lagrange equations. The resulting intrinsic form of the Euler-Lagrange equations are more compact than equations expressed in terms of local coordinates.

Problems, singularities with Euler-Angles

Other attitude representations, such as  exponential coordinates, quaternions, or Euler angles, can also be used following standard descriptions, but each of the representations has a disadvantage of introducing an ambiguity or singularity. Why charts on $SO(3)$ [https://en.wikipedia.org/wiki/Charts_on_SO\(3\)](https://en.wikipedia.org/wiki/Charts_on_SO(3))

Euler Angles

However, the definition of Euler angles is not unique and in the literature many different conventions are used. These conventions depend on the axes about which the rotations are carried out, and their sequence because rotations are not commutative. Therefore, Euler angles are never expressed in terms of the external frame, or in terms of the co-moving rotated body frame, but in a mixture. Other conventions (e.g., rotation matrix or quaternions) are used to avoid this problem.

Manifolds The fundamental object of differential geometry a manifold. A manifold is a mathematical space, a collection of points, that locally resembles Euclidean space near each point. Examples are a plane, a ball, a torus and a sphere. Manifolds are important objects

in mathematics and physics because they allow more complicated structures to be expressed and understood in terms of the relatively well-understood properties of simpler spaces. In Figure 2-3 is illustrated that each point of an n -dimensional manifold has a neighborhood that is homeomorphic to the n -dimensional Euclidean space, meaning that there is a continuous function describing the relation between these spaces.



Figure 2-3: A manifold locally resembles a Euclidean space

A differentiable manifold is a smooth and continuous manifold and is locally similar enough to a linear space to allow to do calculus. One can define directions, tangent spaces, and differentiable functions on such a manifold. Each point of an n -dimensional differentiable manifold has a tangent space, which is an n -dimensional Euclidean space consisting of the tangent vectors of the curves through that point. In Figure 2-4a the manifold \mathbb{S}^2 is represented as a sphere, with a tangent space at point x , denoted by $T_x\mathbb{S}^2$. Taking the derivative at a point on a manifold is equivalent to a tangent vector at that point. Meaning that derivatives are conceptually equivalent to an infinitesimally short tangent vector.



(a) Representation of a manifold with a tangent space



(b) Identity map of $SO(3)$ with Lie Algebra $\mathfrak{so}(3)$

Figure 2-4

Configuration Spaces Rotation matrices are used to provide a global representation of the attitude of a rigid body, by mapping a representation of vectors expressed in $\{\mathcal{B}\}$ to a representation expressed in $\{\mathcal{I}\}$ [10, 11]. The configuration of the \mathbf{QR} attitude is a rotation matrix R in the Special Orthogonal Group $SO(3)$ defined as

$$SO(3) \triangleq \{R \in \mathbb{R}^{3 \times 3} | RR^T = I_{3 \times 3}, \det(R) = 1\} \quad (2-4)$$

$SO(3)$ is the group of all rotations about the origin of a 3-D Euclidean space, which preserves the origin, Euclidean distance and orientation. Every rotation has a unique inverse rotation and the identity map satisfies the definition of a rotation. The elements of *Lie Algebra* $\mathfrak{so}(3)$, a property associated with $SO(3)$, are the elements of the tangent space of $SO(3)$ at the identity element, see Figure 2-4b. These elements define the relation between the rotation R and its derivative \dot{R} , such that

$$\dot{R} = R\hat{\Omega} \quad (2-5)$$

$\mathfrak{so}(3)$ is defined as

$$\mathfrak{so}(3) \triangleq \{U \in \mathbb{R}^{3 \times 3} | U^T = -U\} \quad (2-6)$$

Where a mapping from the angular velocity vector $\Omega \in \mathbb{R}^3$ to $\hat{\Omega} \in \mathfrak{so}(3)$ is defined as [11]

$$\hat{\Omega} = \begin{bmatrix} 0 & -\Omega_3 & \Omega_2 \\ \Omega_3 & 0 & -\Omega_1 \\ -\Omega_2 & \Omega_1 & 0 \end{bmatrix} \quad (2-7)$$

The hat map $\hat{\cdot} : \mathbb{R}^3 \rightarrow \mathfrak{so}(3)$ is an isomorphism between \mathbb{R}^3 and the set of 3×3 skew symmetric matrices.

The configuration space of the load is represented on a 2-sphere, defined as

$$\mathbb{S}^2 \triangleq \{q \in \mathbb{R}^3 | q \cdot q = 1\} \quad (2-8)$$

$$\dot{q} = \omega \times q \quad (2-9)$$

where ω is the angular velocity of the suspended load.

Local coordinates Euler angles are kinematically singular since the transformation from their time rates of change to the angular velocity vector is not globally defined. Furthermore, when angular errors are large, the difference in Euler angles is no longer a good metric to define the orientation error. Local coordinates often require symbolic computational tools due to complexity of multi-body systems. Hence, the error is rather written as the required rotation to get from the current to a desired orientation. As a result, the equations of motion and the control systems can be developed on a configuration manifold in a coordinate-free, compact, unambiguous manner, while singularities of local parameterization are avoided.

To illustrate the difference in configuration spaces, an example is given of a 2-link arm, where the configuration can be expressed by 2 coordinates, see in Figure 2-5. Figure 2-5b represents the configuration space as a Cartesian space, where the same dots represent one of the many identical configurations. This shows that this representation suffers from singularities caused by multiple points in one representation being mapped onto a single point in another representation. Figure 2-5c shows the configuration space as a *torus*, a manifold where every configuration is mapped uniquely onto the manifold.

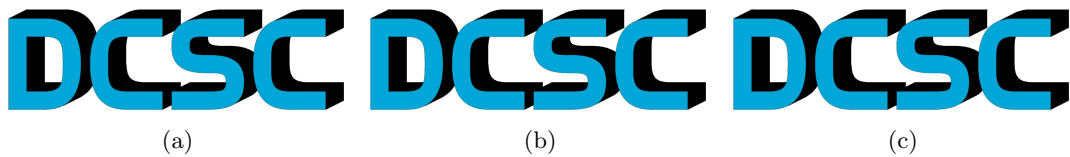


Figure 2-5: Configuration Space of a 2-link arm

2-3 Quadrotor-Load Model



In this section the model dynamics are obtained with the concepts of differential geometry. The dynamics of the QR-Load system can be described on nonlinear manifolds. The focus lies on the subsystem where the cable tension is considered to be non-zero.

The Quadrotor-Load model is shown in Figure 2-6, where the unit vector q gives the direction from the QR to the Load expressed in $\{\mathcal{B}\}$.

The configuration of the QR can be described by the location of its **com!** and its attitude, described in Euclidean space $x_Q \in \mathbb{R}^3$ and in a nonlinear space $R \in SO(3)$ respectively. Whereas the configuration of the load can also be described by its location and attitude, described in Euclidean space $x_L \in \mathbb{R}^3$ and on a two-sphere $q \in \mathbb{S}^2$.

The position of the QR and Load are related by

$$x_Q = x_L - Lq \quad (2-10)$$

where L is the length of the cable.

The attitude kinematics equation is given by

$$\dot{R} = R\hat{\Omega} \quad (2-11)$$

where $\Omega \in \mathbb{R}^3$ is the angular velocity represented in the body fixed frame, defined as Equation 2-7.

Variations on manifolds *****

Looking at the variations on manifolds

This is different from traditional mechanics



Figure 2-6: Quadrotor-Load model representation

To develop the Euler-Lagrange equations for mechanical systems that evolve on a Lie group, an approach developed by [3, 12, 13, 14] is used, which is based on Hamilton's principle.

The action integral is defined as

$$S = \int_{t_1}^{t_2} \mathcal{L} dt \quad (2-12)$$

where $\mathcal{L} = \mathcal{T} - \mathcal{U}$ is the Lagrangian of the system, where \mathcal{T}, \mathcal{U} are the kinetic and potential energy, respectively. Hamilton's principle of least action states that the path a conservative

mechanical system takes between two configurations at time t_1 and t_2 , is the one for which Equation 2-12 is an extremum, stated as

$$\delta S = \int_{t_1}^{t_2} \delta \mathcal{L} dt = 0 \quad (2-13)$$

where $\delta \mathcal{L}$ is the variation of the Lagrangian. For systems with non-conservative forces and moments, Equation 2-13 is extended to

$$\delta S = \int_{t_1}^{t_2} (\delta W + \delta \mathcal{L}) dt = 0 \quad (2-14)$$

where δW is the virtual work. Equation 2-14 is applied to the QR-Load system, where the configuration manifold is $\mathbb{R}^3 \times \mathbb{S}^2 \times SO(3)$. With the following states

$$\mathbf{x} = [x_L \quad \dot{x}_L \quad q \quad \omega \quad R \quad \Omega]^T \quad (2-15)$$

Rigid Body Attitude Dynamics evolve on $SE(3)$.

$$J\dot{\Omega} + \Omega \times J\Omega = mg\rho \times R^T e_3 + u \quad (2-16)$$

$$\dot{R} = R\hat{\Omega} \quad (2-17)$$

The equations of motion for a rigid body with configuration $SE(3)$ are given by the *Newton-Euler equations* [11]:

$$\begin{bmatrix} mI & 0 \\ 0 & \mathcal{I} \end{bmatrix} \begin{bmatrix} \dot{v}^b \\ \dot{\omega}^b \end{bmatrix} + \begin{bmatrix} \omega^b \times m v^b \\ \omega^b \times \mathcal{I} \omega^b \end{bmatrix} = F^b \quad (2-18)$$

where m is the mass of the body, \mathcal{I} is the inertia tensor, and $V^b = (v^b, \omega^b)$ and F^b represent the instantaneous body velocity and applied body wrench.

The load dynamics evolve on \mathbb{S}^2 . Based on [14].

2-4 Classical Modeling

This section describes the derivation of the  model by using classical modeling techniques.

Reference ??

When assuming small angle maneuvers, *Euler-angles* can be used to locally parameterize the orientation of the body-fixed reference coordinate frame with respect to the inertial reference coordinate frame. Simple linear controllers are often based on a linearized dynamical model, applying this small angles assumption.

From Newton's law follows

$$\begin{aligned} \dot{x}_Q &= v_Q \\ m_Q \dot{v}_Q &= f R e_3 - m_Q g e_3 - T q \\ \dot{x}_L &= v_L \\ m_L \dot{v}_L &= -m_L g e_3 + T q \end{aligned} \quad (2-19)$$

Because the Euler-Angles are used, a function is required that maps a vector of the Z-X-Y Euler angles to its rotation matrix $R \in SO(3)$, which is denoted as [15]

$$R_{312}(\phi, \theta, \psi) = \begin{bmatrix} c_\psi c_\theta - s_\phi s_\psi s_\theta & -c_\phi s_\psi & c_\psi s_\theta + c_\theta s_\phi s_\psi \\ c_\theta s_\psi + c_\psi s_\phi s_\theta & c_\phi c_\psi & s_\psi s_\theta - c_\psi c_\theta s_\phi \\ -c_\phi s_\theta & s_\phi & c_\phi c_\theta \end{bmatrix} \quad (2-20)$$

The Z-X-Y Euler angles to model the rotation can be seen in Figure 2-7. The first rotation by yaw angle ψ is around the z-axis of $\{\mathcal{I}\}$. Next is the rotation by roll angle ϕ , and the last rotation is by pitch angle θ .

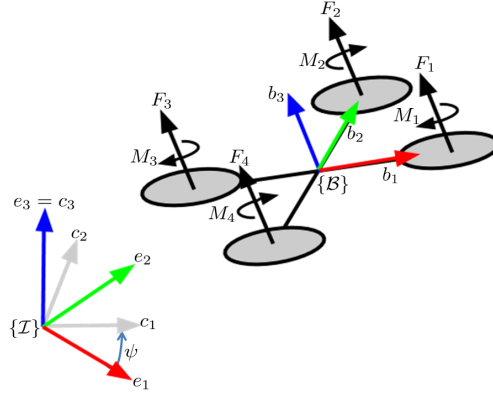


Figure 2-7: Quadrotor-Load model representation

The unit vector q from the QR to the load is represented in $\{\mathcal{B}\}$. Define ϕ_L as the yaw-rotation of the load around the z-axis of $\{\mathcal{B}\}$ and θ_L as the angle between the cable and the z-axis of $\{\mathcal{B}\}$, see Figure 2-8.

$$q = \begin{bmatrix} s_{\theta_L} c_{\phi_L} \\ s_{\theta_L} s_{\phi_L} \\ c_{\theta_L} \end{bmatrix} \quad (2-21)$$



Figure 2-8

Differentiating Equation (2-10) and (2-21) gives

$$\ddot{x}_L = \ddot{x}_Q - \ddot{q}L$$

$$\ddot{q} = \begin{bmatrix} \ddot{\theta}_L c_{\theta_L} c_{\phi_L} - \ddot{\phi}_L s_{\theta_L} s_{\phi_L} - \dot{\phi}_L^2 s_{\theta_L} c_{\phi_L} - \dot{\theta}_L^2 s_{\theta_L} c_{\phi_L} - 2\dot{\theta}_L \dot{\phi}_L c_{\theta_L} s_{\phi_L} \\ \ddot{\theta}_L c_{\theta_L} s_{\phi_L} + \ddot{\phi}_L s_{\theta_L} c_{\phi_L} - \dot{\phi}_L^2 s_{\theta_L} s_{\phi_L} - \dot{\theta}_L^2 s_{\theta_L} s_{\phi_L} + 2\dot{\theta}_L \dot{\phi}_L c_{\theta_L} c_{\phi_L} \\ -\ddot{\theta}_L s_{\theta_L} - \ddot{\phi}_L^2 c_{\theta_L} \end{bmatrix} \quad (2-22)$$

$$\ddot{x}_Q = \frac{1}{m_Q} (f(c_\psi s_\theta + c_\theta s_\phi s_\psi) - T s_{\theta_L} c_{\psi_L})$$

$$\ddot{y}_Q = \frac{1}{m_Q} (f(s_\psi s_\theta - c_\psi c_\theta s_\phi) - T s_{\theta_L} s_{\psi_L}) \quad (2-23)$$

$$\ddot{z}_Q = \frac{1}{m_Q} (f(c_\phi c_\theta) - T c_{\theta_L}) - g$$

$$\ddot{\psi} = \ddot{\tau}_\psi \quad (2-24)$$

$$\ddot{\theta} = \ddot{\tau}_\theta \quad (2-25)$$

$$\ddot{\phi} = \ddot{\tau}_\phi \quad (2-26)$$

2-5 Stability Analysis

Lyapunov Analysis on $SO(3) \times R^3$ and $S^2 \times R^3$ Closed-loop full-attitude dynamics evolve on the non-Euclidean manifold $SO(3) \times R^3$, while closed-loop reduced-attitude dynamics evolve on the non-Euclidean manifold $S^2 \times R^3$. Since these manifolds are locally Euclidean, local stability properties of a closed-loop equilibrium solution can be assessed using standard Lyapunov methods. In addition, the LaSalle invariance result and related Lyapunov results apply to closed-loop vector fields defined on these manifolds. However, since the manifolds $SO(3)$ and S^2 are compact, the radial unboundedness assumption cannot be satisfied; consequently, global asymptotic stability cannot follow from a Lyapunov analysis on Euclidean spaces [40], and therefore must be analyzed in alternative ways [19]–[23]. [10, p.43]

2-6 Summary

Compact, unambiguous, globally defined,

Pro/Cons of Classical Modeling Techniques vs Geometric Modeling

Linearized model/State Space model vs. Geometric modeling

Geometric Mechanics/Lie Groups/Lie Algebra is used in order to represent the dynamics of the system onto the nonlinear configuration manifold $SE(3)$

Advantage of this method is

Enables to model on

That type of control is discussed in the next chapter

Chapter 3

Geometric Control Design

Geometric Control Theory explores the application of differential geometric techniques to systems control. The objective is to express both the dynamics and its control inputs on manifolds instead of on local charts. Geometric control theory is the study of how the geometry of the state space influences controls problems. This includes local properties like curvature, and global properties like the number of ‘holes’ in the space (sphere vs doughnut).

Geometric Control is based on a coordinate-free representation of the dynamics, where the equations of motion are compact, unambiguous and singularity free. Globally defined (no singularities!). Therefore, one can build almost globally attractive controllers

Attitude control systems naturally evolve on non-linear configurations such as \mathbb{S}^2 and $SO(3)$. Tracking control system can be developed on $SO(3)$, therefore it avoids singularities of Euler-Angles.

Global nonlinear dynamics of various classes of closed loop attitude control systems have been studied in recent years [?]. In contrast to hybrid control systems [16], **complicated reachability set analysis is not required** to guarantee safe switching between different flight modes, as the region of attraction for each flight mode covers the configuration space almost globally.

3-1 Backstepping Control

A backstepping approach, or cascade control, is a Lyapunov based technique to design the control of nonlinear dynamical systems, while ensuring Lyapunov stability. The principle is to create a cascaded structure by starting with a stable system as a base, then ”stepping back” from the base to add a control loop around it that stabilizes the added subsystem. This is repeated until the the final external control is reached. The control law is designed by using states as virtual control signals. Each outer loop outputs a virtual control input for the inner loop in order to control the outer loop.



Figure 3-1: Backstepping Control representation of the QR

A backstepping control approach is common for QRs [?] and can be seen in Figure 3-1. The lowest level has the highest bandwidth and is in control of the rotor rotational speeds. The next level controls the QR attitude, and the top level controls the QR position.

Because the QR has only four actuators, it is not possible to control all DOFs of the QR-Load system. Therefore, different flight modes are specified in which parts of the DOFs are controlled. The same backstepping approach allows different flight modes that are defined as follows

- QR Attitude Controlled Mode
 - Track a QR attitude command $R_d(t)$ and a heading direction $b_{1_d}(t)$
- Load Attitude Controlled Mode
 - Track a load attitude command $q_d(t)$
- Load Position Controlled Mode
 - Track a load position $x_{L,d}(t)$



Figure 3-2: Backstepping Control representation of the QR-Load system

3-2 Configuration Errors

Most of nonlinear dynamics and control problems are studied in a linear space.

$$\dot{x} = \mathbf{f}(t, x, u), \quad x \in \mathbb{R}^n, u \in \mathbb{R}^m, \mathbf{f}: \mathbb{R}^{n+m+1} \rightarrow \mathbb{R}^n \quad (3-1)$$

In control systems engineering, the underlying geometric features of a dynamic system are often not considered carefully. For example, many control systems are developed for the standard form of ordinary differential equations, namely $\dot{x} = f(x, u)$, where the state and the control input are denoted by x and u . It is assumed that the state and the control input lie in

Euclidean spaces, and the system equations are defined in terms of smooth functions between Euclidean spaces. However, for many interesting mechanical systems, the configuration space cannot be expressed globally as a Euclidean space.

Before the controllers are described, the configuration functions are defined as in [8]. These functions describe the error on the manifolds $SO(3)$ and \mathbb{S}^2 , which describe the configuration spaces for the QR attitude and the load attitude, respectively.

Define errors associated with the attitude dynamics of the QR. The attitude and angular velocity tracking error should be carefully chosen as they evolve on the tangent bundle of $SO(3)$. [?]

The error function on $SO(3)$ is chosen to be [17]

$$\Psi_R(R, R_d) = \frac{1}{2} \text{tr} [I - R_d^T R] \quad (3-2)$$

The error function on \mathbb{S}^2 is chosen to be

$$\Psi_q \quad (3-3)$$

The tracking error functions on the tangent space of $SO(3)$, denoted by $TSO(3)$ are defined as

$$e_R \quad (3-4)$$

$$e_\Omega \quad (3-5)$$

The tracking error functions on the tangent space of \mathbb{S}^2 , denoted by $T\mathbb{S}^2$ are defined as

$$e_q \quad (3-6)$$

$$e_{\dot{q}} \quad (3-7)$$

The tracking errors for position and velocity are defined as

$$e_x = x - x_d \quad (3-8)$$

$$e_v = v - v_d \quad (3-9)$$

$$\text{where, } v_d = \dot{x}_d \quad (3-10)$$

where $x_d(t) \in \mathbb{R}^3$ is a smooth desired load position.



Figure 3-3

3-3 Quadrotor Attitude Tracking

This control problem has been addressed in various works *****

The most inner loop controls the attitude of the QR.

Attitude control problem is the inner loop of the control design. This inner loop must guarantee stability of the QR.

Must track reference attitude.

The attitude and angular velocity tracking error should be carefully chosen as they evolve on the tangent bundle of the nonlinear space $SO(3)$. [17]

Why? Appendix [17], and [8]?

The moment consists of a proportional term, a derivative term and a canceling term, and is defined as follows

$$M = \frac{1}{\epsilon^2} k_R e_R - \frac{1}{\epsilon} k_\Omega e_\Omega + \Omega \times J_Q \Omega - J_Q (\hat{\Omega} R^T R_d \Omega_d - R^T R_d \dot{\Omega}_d) \quad (3-11)$$

Asymptotic tracking of the quadrotor attitude does not require specification of the thrust magnitude. As an auxiliary problem, the thrust magnitude can be chosen in many different ways to achieve an additional translational motion objective. For example, it can be used to asymptotically track a quadrotor altitude command [28]. Since the translational motion of the quadrotor UAV can only be partially controlled; this flight mode is most suitable for short time periods where an attitude maneuver is to be completed. [19]

Control input [14]

$$u = -k_R e_R - k_\Omega \Omega - mg \rho \times R^T e_3 \quad (3-12)$$

Insert into Equation 2-16; closed loop dynamics are given by

$$J \dot{\Omega} = -\Omega \times J \Omega - k_R e_R - k_\Omega \Omega \quad (3-13)$$

$$\dot{R} = R \hat{\Omega} \quad (3-14)$$

3-4 Load Attitude Tracking

Tracks load attitude reference. Outputs attitude reference to attitude controller.



Figure 3-4

How is the controller built.

Dependent of what values? How to choose parameters.

$$R = \quad (3-15)$$

3-5 Load Position Tracking

Tracks load position reference. Outputs load attitude reference.

$$q = \quad (3-16)$$



Figure 3-5

3-6 Parameter- and State Estimation

How to choose parameters and how to select gains for errors

How to estimate states?

What parameters must be

Refer to Lyapunov stability analysis [8]

3-7 Summary

What is Geometric Control?

Why Geometric Control?

Control design will be based on Nonlinear Geometric Control

The proposed control system is robust to switching conditions since each flight mode has almost global stability properties, and it is straightforward to design a complex maneuver of a QR. [20] Where are the Error functions based on?

Form bridge between Geometric Control and Hybrid Control

Why Hybrid Control?

Parameter Estimation can be done by

State Estimation can be done by

Drawback: assumes all states to be known

Model based. What if analytical model is not accurate?

Experiments and Results

This chapter describes experiments that are done in order to investigate the abilities and performance of a nonlinear Geometric Control design. Different cases are defined that describe tracking objectives in order to test the performance of both a simple LQR control design and a nonlinear Geometric Control design. These results are presented, and this chapter ends with a conclusion based on these results.

4-1 Setup

Model parameters The simulations are developed using Matlab and Simulink, using the following system parameters.

$$\begin{array}{lll} J = & d = & m_L = \\ m_Q = & c_{\tau f} = & l_L = \end{array}$$

LQR Control LQR control is based on small angle assumption. Therefore, a traditional modeling method may represent the rotation matrix with a local coordinate system, for example with a Euler Angle parameterization. An LQR control design is based on a linearized model of the system, which is derived in Section A-2, and is shown in Figure 4-1.



Figure 4-1: LQR control design

The tuning parameters of the LQR controller are chosen as follows

$$A = [\text{content...}] \quad (4-1)$$

$$B = [\text{content...}] \quad (4-2)$$

$$C = [\text{content...}] \quad (4-3)$$

where the state \mathbf{x} and input u are defined as

$$\mathbf{x} = \begin{bmatrix} \mathbf{q} \\ \dot{\mathbf{q}} \end{bmatrix} \quad (4-4)$$

$$\mathbf{q} = [x \ y \ z \ \phi \ \theta \ \psi \ \theta_L \ \psi_L]^T \quad (4-5)$$

$$\dot{\mathbf{q}} = [\dot{x} \ \dot{y} \ \dot{z} \ \dot{\phi} \ \dot{\theta} \ \dot{\psi} \ \dot{\theta}_L \ \dot{\psi}_L]^T \quad (4-6)$$

$$u = [f \ M_\phi \ M_\theta \ M_\psi]^T \quad (4-7)$$

Geometric Control The controller gains in Equations 3-11,3-15,3-16 are chosen to be

$$\begin{aligned} k_R &= k_q = k_x = \\ k_\Omega &= k_\omega = k_v = \end{aligned}$$

4-1-1 Command Filtering

Consequence of backstepping control is that inner control loops depend on the the output of outer control loops. The controllers are functions of these generated outputs and their derivatives. This can be calculated analytically, which can be tedious or by estimating with the use of a Command Filter as explained by [?]

A command filter is implemented to compute $\dot{R}_c, \ddot{R}_c, \dot{q}_c, \ddot{q}_c$, the virtual control command to stabilize the loop within. [?]

Examples from [21] and [22].

Easy implementation. Less computational effort.

Less accurate, because filters high frequency signals.

The load attitude controller generates a commanded QR attitude R_c and its derivative \dot{R}_c . In the same fashion, the load position controller generates a commanded load attitude q_c and its derivative \dot{q}_c . The controllers are functions of these commanded signals and their derivatives. Instead of analytic differentiation of these signals, they are obtained by integration by applying a third order low pass filter to the original signals R_c^o and q_c^o . The transfer function of the original commanded input signal X_c^o and the filtered output X_c has the form

$$\frac{X_c(s)}{X_c^o(s)} = H(s) = \frac{\omega_{n1}}{s + \omega_{n1}} \cdot \frac{\omega_{n2}^2}{s^2 + 2\zeta\omega_{n2}s + \omega_{n2}^2} \quad (4-8)$$

Where x_c is the filtered signal, ζ the damping ratio and ω_n the undamped natural frequency. See Figure 4-2. The state space implementation of this third order filter is [22]

$$\dot{x}_1 = x_2 \quad (4-9)$$

$$\dot{x}_2 = x_3 \quad (4-10)$$

$$\dot{x}_3 = -(2\zeta\omega_{n2} + \omega_{n1})x_3 - (2\zeta\omega_{n1}\omega_{n2} + \omega_{n2}^2)x_2 - (\omega_{n1}\omega_{n2}^2)(x_1 - x_c^o) \quad (4-11)$$

where $x_1 = x_c$, $x_2 = \dot{x}_c$ and $x_3 = \ddot{x}_c$.



Figure 4-2: Representation of the command filter

$$\frac{x_c}{x_c^o} = \frac{\omega_{n1}}{s + \omega_{n1}} \cdot \frac{\omega_{n2}^2}{s^2 + 2\zeta\omega_{n2}s + \omega_{n2}^2} \quad (4-12)$$

$$\Rightarrow x_c''' = -(2\zeta\omega_{n2} + \omega_{n1})x_c'' - (2\zeta\omega_{n1}\omega_{n2} + \omega_{n2}^2)x_c' - (\omega_{n1}\omega_{n2}^2)(x_c - x_c^o) \quad (4-13)$$

4-2 Experiments

LQR is an optimal control strategy and will be used to compare its result to a Nonlinear Geometric Controller.

4-2-1 Performance Criteria

Performance that can be evaluated for different cases can be specified as the following items.

- Step Response
 - Settling time (if swing minimization is important)
 - Rising time (important if time critical)
 - Overshoot (if max swing is critical)
 - Steady state error / swing of load (if accuracy is important)
 - Max load angle
- Disturbance Rejection
- Trajectory tracking
 - Can we minimize time, while minimizing position error (All Cases)
 - Minimum position error (All Cases)

- Maximum amplitude/frequency of wave with respect to stability (Case B)
- Computational Effort (?)

Explain cases, why interesting and what can be expected?

4-2-2 Case A

4-2-3 Case B

4-2-4 Case C



Figure 4-3: Cases of which the performance could be evaluated

4-3 Results

4-3-1 Case A

4-3-2 Case B

4-3-3 Case C

4-4 Conclusion

Conclusions and Future Work

5-1 Summary and Conclusions

5-2 Recommendations for Future Work

Model Validation; now it's estimation/copied from other work
System Identification

5-2-1 Modeling Constraints

There are several techniques to handle input saturation, the most popular ones are anti-windup techniques. Back-calculation is such a method for PID to activate the integrator, is this possible for NL control?

[4] includes uncertainties in the translational dynamics and rotational dynamics. Out of the scope, might be interesting.

5-2-2 Hybrid Modeling

Switching between several flight modes yields autonomous acrobatic maneuvers. Robust to switching conditions ***why?

[23]

5-2-3 Trajectory Generation

Minimum Snap Trajectory Generation

Trajectory can be generated by solving a **QP!** via minimum snap generation.

Problem in smaller 4-D space instead of 12-D, with help of differential flatness. Explain differential flatness and its usefulness.

Is able to include constraints in **QP!**.

[\[18\]](#)

Obstacle avoidance

Appendix A

Appendix

A-1 Derivation of Equations of motion

A-1-1 Load Dynamics

Let x_{CM} denote the position of the center of mass of the combined Quadrotor-Load system, expressed in $\{\mathcal{I}\}$. Which can be found by

$$\begin{aligned} m_Q(x_Q - x_{CM}) + m_L(x_L - x_{CM}) &= 0 \\ (m_Q + m_L)x_{CM} &= m_Q x_Q + m_L x_L \end{aligned} \tag{A-1}$$

Applying the laws of motion to (A-1) and inserting (2-10) gives the

$$\begin{aligned} (m_Q + m_L)\ddot{x}_{CM} &= fRe_3 - (m_Q + m_L)ge_3 \\ (m_Q + m_L)(\ddot{x}_L + ge_3) &= fRe_3 + m_Q L\ddot{q} \end{aligned} \tag{A-2}$$

A-2 Derivation of LQR controller

A-2-1 Modeling

From Newton's laws follows

$$x_Q = fRe_3 - m_Q ge_3 - Tq \tag{A-3}$$

$$x_L = -m_L ge_3 + Tq \tag{A-4}$$

x_Q and x_L are related by

$$x_L = x_Q + Lq \tag{A-5}$$

$$\begin{aligned}\ddot{x} &= \\ \ddot{y} &= \\ \ddot{z} &= \end{aligned} \tag{A-6}$$

$$\begin{aligned}\ddot{\phi} &= \\ \ddot{\theta} &= \\ \ddot{\psi} &= \end{aligned} \tag{A-7}$$

$$\begin{aligned}\ddot{\phi}_L &= \\ \ddot{\theta}_L &= \end{aligned} \tag{A-8}$$

A-2-2 Controller

$$\mathbf{x} = \begin{bmatrix} \mathbf{q} \\ \dot{\mathbf{q}} \end{bmatrix} \tag{A-9}$$

$$\mathbf{q} = [x \ y \ z \ \phi \ \theta \ \psi \ \theta_L \ \psi_L]^T \tag{A-10}$$

$$\dot{\mathbf{q}} = [\dot{x} \ \dot{y} \ \dot{z} \ \dot{\phi} \ \dot{\theta} \ \dot{\psi} \ \dot{\theta}_L \ \dot{\psi}_L]^T \tag{A-11}$$

$$\mathbf{u} = [f \ M_\phi \ M_\theta \ M_\psi]^T \tag{A-12}$$

$$\dot{\mathbf{x}} = \mathbf{A}\mathbf{x} + \mathbf{B}\mathbf{u} \tag{A-13}$$

$$y = \mathbf{C}\mathbf{x} + \mathbf{D}\mathbf{u} \tag{A-14}$$

$$\dot{\mathbf{x}} = \mathbf{f}(\mathbf{x}, \mathbf{u}) \tag{A-15}$$

By linearizing Equations A-6,A-7,A-8 follows

$$\ddot{x} = -\frac{f}{m} \tag{A-16}$$

$$\ddot{y} = \tag{A-17}$$

$$\ddot{z} = \tag{A-18}$$

The mathematical model is linearized around the following operating points

$$\bar{\mathbf{x}} = [\bar{x} \ \bar{y} \ \bar{z} \ \mathbf{0}_{1 \times 13}]^T \tag{A-19}$$

$$\bar{\mathbf{u}} = [(m_Q + m_L)g \ 0 \ 0 \ 0]^T \tag{A-20}$$

Assuming small angles, the following holds

$$\text{for } \gamma = \phi, \theta, \psi, \theta_L, \psi_L \quad (\text{A-21})$$

$$\sin(\gamma) \simeq \gamma \quad (\text{A-22})$$

$$\cos(\gamma) \simeq 1 \quad (\text{A-23})$$

$$\dot{\gamma} \simeq 0 \quad (\text{A-24})$$

$$F \simeq (m_Q + m_L)g \quad (\text{A-25})$$

$$A = \frac{\partial \mathbf{f}(x, u)}{\partial x} \Big|_{x=\bar{x}, u=\bar{u}} \quad (\text{A-26})$$

$$B = \frac{\partial \mathbf{f}(x, u)}{\partial u} \Big|_{x=\bar{x}, u=\bar{u}} \quad (\text{A-27})$$

$$u = -K [\mathbf{x}_{des}(t) - \mathbf{x}(t)] \quad (\text{A-28})$$

A-3 MATLAB code

$$Testequation \quad (\text{A-29})$$

A-3-1 A MatlabListing

```
%
% Comment
%
n=10;
for i=1:n
    disp('Ok');
end
```

1

6

Bibliography

- [1] M. Bangura and R. Mahony, “Real-time model predictive control for quadrotors,” in *IFAC Proceedings Volumes (IFAC-PapersOnline)*, vol. 19, pp. 11773–11780, 2014.
- [2] R. P. K. Jain and T. Keviczky, “MSc Thesis: Transportation of Cable Suspended Load using Unmanned Aerial Vehicles: A Real-time Model Predictive Control approach,” 2015.
- [3] T. Lee, *Computational Geometric Mechanics and Control of Rigid Bodies*. PhD thesis, The University of Michigan, 2008.
- [4] F. Goodarzi, D. Lee, and T. Lee, “Geometric nonlinear PID control of a quadrotor UAV on SE (3),” *Control Conference (ECC), 2013 European*, pp. 3845–3850, 2013.
- [5] K. Sreenath, T. Lee, and V. Kumar, “Geometric control and differential flatness of a quadrotor UAV with a cable-suspended load,” in *Proceedings of the IEEE Conference on Decision and Control*, pp. 2269–2274, 2013.
- [6] S. Tang and V. Kumar, “Mixed Integer Quadratic Program Trajectory Generation for a Quadrotor with a Cable-Suspended Payload,” *IEEE International Conference on Robotics and Automation (ICRA)*, pp. 2216–2222, 2015.
- [7] W. M. Boothby, *An Introduction to Differentiable Manifolds and Riemannian Geometry*. 2003.
- [8] F. Bullo and A. D. Lewis, *Geometric control of mechanical systems: modeling, analysis, and design for simple mechanical control systems*. Springer, 2005.
- [9] V. Jurdjevic, *Geometric Control Theory*. Cambridge: Cambridge University Press, 1997.
- [10] N. Chaturvedi, A. Sanyal, and N. McClamroch, “Rigid-Body Attitude Control,” *IEEE Control Systems*, vol. 31, no. 3, pp. 30–51, 2011.
- [11] R. M. Murray, Z. Li, and S. S. Sastry, *A Mathematical Introduction to Robotic Manipulation*, vol. 29. 1994.

- [12] T. L. T. Lee, N. McClamroch, and M. Leok, "A lie group variational integrator for the attitude dynamics of a rigid body with applications to the 3D pendulum," *Proceedings of 2005 IEEE Conference on Control Applications, 2005. CCA 2005.*, pp. 962–967, 2005.
- [13] T. Lee, M. Leok, and N. H. McClamroch, "Lagrangian mechanics and variational integrators on two-spheres," *International Journal for Numerical Methods in Engineering*, vol. 79, no. 9, pp. 1147–1174, 2009.
- [14] T. Lee, M. Leok, and N. H. McClamroch, "Stable Manifolds of Saddle Points for Pendulum Dynamics on S^2 and $SO(3)$," p. 9, 2011.
- [15] R. Mahony, V. Kumar, and P. Corke, "Multirotor Aerial Vehicles: Modeling, Estimation, and Control of Quadrotor," *IEEE Robotics & Automation Magazine*, vol. 19, no. 3, pp. 20–32, 2012.
- [16] J. H. Gillula, H. Huang, M. P. Vitus, and C. J. Tomlin, "Design of guaranteed safe maneuvers using reachable sets: Autonomous quadrotor aerobatics in theory and practice," in *Proceedings - IEEE International Conference on Robotics and Automation*, pp. 1649–1654, 2010.
- [17] T. Lee, M. Leok, and N. H. McClamroch, "Geometric Tracking Control of a Quadrotor UAV on $SE(3)$," *49th IEEE Conference on Decision and Control*, no. 3, pp. 5420–5425, 2010.
- [18] D. Mellinger and V. Kumar, "Minimum snap trajectory generation and control for quadrotors," in *Proceedings - IEEE International Conference on Robotics and Automation*, pp. 2520–2525, 2011.
- [19] F. A. Goodarzi, "Geometric Nonlinear Controls for Multiple Cooperative Quadrotor UAVs Transporting a Rigid Body," no. December 2009, 2015.
- [20] T. Lee, M. Leok, and N. McClamroch, "Control of complex maneuvers for a quadrotor UAV using geometric methods on $SE(3)$," *arXiv*, 2010.
- [21] J. A. Farrell, M. Polycarpou, M. Sharma, and W. Dong, "Command Filtered Backstepping," pp. 1923–1928, 2008.
- [22] V. Djapic, J. Farrell, and W. Dong, "Land vehicle control using a command filtered backstepping approach," *Proceedings of the American Control Conference*, pp. 2461–2466, 2008.
- [23] S. Tang, "Aggressive Maneuvering of a Quadrotor with a Cable-Suspended Payload," tech. rep., University of Pennsylvania Philadelphia, Pennsylvania, 2014.

Bibliography

- [1] M. Bangura and R. Mahony, “Real-time model predictive control for quadrotors,” in *IFAC Proceedings Volumes (IFAC-PapersOnline)*, vol. 19, pp. 11773–11780, 2014.
- [2] R. P. K. Jain and T. Keviczky, “MSc Thesis: Transportation of Cable Suspended Load using Unmanned Aerial Vehicles: A Real-time Model Predictive Control approach,” 2015.
- [3] T. Lee, *Computational Geometric Mechanics and Control of Rigid Bodies*. PhD thesis, The University of Michigan, 2008.
- [4] F. Goodarzi, D. Lee, and T. Lee, “Geometric nonlinear PID control of a quadrotor UAV on SE (3),” *Control Conference (ECC), 2013 European*, pp. 3845–3850, 2013.
- [5] K. Sreenath, T. Lee, and V. Kumar, “Geometric control and differential flatness of a quadrotor UAV with a cable-suspended load,” in *Proceedings of the IEEE Conference on Decision and Control*, pp. 2269–2274, 2013.
- [6] S. Tang and V. Kumar, “Mixed Integer Quadratic Program Trajectory Generation for a Quadrotor with a Cable-Suspended Payload,” *IEEE International Conference on Robotics and Automation (ICRA)*, pp. 2216–2222, 2015.
- [7] W. M. Boothby, *An Introduction to Differentiable Manifolds and Riemannian Geometry*. 2003.
- [8] F. Bullo and A. D. Lewis, *Geometric control of mechanical systems: modeling, analysis, and design for simple mechanical control systems*. Springer, 2005.
- [9] V. Jurdjevic, *Geometric Control Theory*. Cambridge: Cambridge University Press, 1997.
- [10] N. Chaturvedi, A. Sanyal, and N. McClamroch, “Rigid-Body Attitude Control,” *IEEE Control Systems*, vol. 31, no. 3, pp. 30–51, 2011.
- [11] R. M. Murray, Z. Li, and S. S. Sastry, *A Mathematical Introduction to Robotic Manipulation*, vol. 29. 1994.

- [12] T. L. T. Lee, N. McClamroch, and M. Leok, "A lie group variational integrator for the attitude dynamics of a rigid body with applications to the 3D pendulum," *Proceedings of 2005 IEEE Conference on Control Applications, 2005. CCA 2005.*, pp. 962–967, 2005.
- [13] T. Lee, M. Leok, and N. H. McClamroch, "Lagrangian mechanics and variational integrators on two-spheres," *International Journal for Numerical Methods in Engineering*, vol. 79, no. 9, pp. 1147–1174, 2009.
- [14] T. Lee, M. Leok, and N. H. McClamroch, "Stable Manifolds of Saddle Points for Pendulum Dynamics on S^2 and $SO(3)$," p. 9, 2011.
- [15] R. Mahony, V. Kumar, and P. Corke, "Multirotor Aerial Vehicles: Modeling, Estimation, and Control of Quadrotor," *IEEE Robotics & Automation Magazine*, vol. 19, no. 3, pp. 20–32, 2012.
- [16] J. H. Gillula, H. Huang, M. P. Vitus, and C. J. Tomlin, "Design of guaranteed safe maneuvers using reachable sets: Autonomous quadrotor aerobatics in theory and practice," in *Proceedings - IEEE International Conference on Robotics and Automation*, pp. 1649–1654, 2010.
- [17] T. Lee, M. Leok, and N. H. McClamroch, "Geometric Tracking Control of a Quadrotor UAV on $SE(3)$," *49th IEEE Conference on Decision and Control*, no. 3, pp. 5420–5425, 2010.
- [18] D. Mellinger and V. Kumar, "Minimum snap trajectory generation and control for quadrotors," in *Proceedings - IEEE International Conference on Robotics and Automation*, pp. 2520–2525, 2011.
- [19] F. A. Goodarzi, "Geometric Nonlinear Controls for Multiple Cooperative Quadrotor UAVs Transporting a Rigid Body," no. December 2009, 2015.
- [20] T. Lee, M. Leok, and N. McClamroch, "Control of complex maneuvers for a quadrotor UAV using geometric methods on $SE(3)$," *arXiv*, 2010.
- [21] J. A. Farrell, M. Polycarpou, M. Sharma, and W. Dong, "Command Filtered Backstepping," pp. 1923–1928, 2008.
- [22] V. Djapic, J. Farrell, and W. Dong, "Land vehicle control using a command filtered backstepping approach," *Proceedings of the American Control Conference*, pp. 2461–2466, 2008.
- [23] S. Tang, "Aggressive Maneuvering of a Quadrotor with a Cable-Suspended Payload," tech. rep., University of Pennsylvania Philadelphia, Pennsylvania, 2014.

Nomenclature

ω_i Angular velocity of rotor i around its axis, $i = \{1, 2, 3, 4\}$

$\tau_{drag,i}$ Drag moment generated by each propellor

$\{\mathbf{b}_1, \mathbf{b}_2, \mathbf{b}_3\}$ Unit vectors along the axes of $\{\mathcal{B}\}$

$\{\mathbf{c}_1, \mathbf{c}_2, \mathbf{c}_3\}$ Unit vectors along the axes of $\{\mathcal{C}\}$

$\{\mathbf{e}_1, \mathbf{e}_2, \mathbf{e}_3\}$ Unit vectors along the axes of $\{\mathcal{I}\}$

$\{\mathcal{B}\}$ Body Frame

$\{\mathcal{C}\}$ Intermediary Frame

$\{\mathcal{I}\}$ Inertial World Frame

b Thrust factor

d Drag factor

L Length of the cable

q Unit vector from Quadrotor to Load

x_L Position of the of the Quadrotor CM

x_Q Position of the of the Quadrotor CM

x_{CM} Position CM of Quadrotor-Load system

A-4 Figures

Acronyms

QR	Quadrotor
UAV	Unmanned Aerial Vehicle
CoM	Center of Mass
DOF	Degree of Freedom
PID controller	Proportional-Integral-Derivative Controller
MPC	Model Predictive Control
Nonlinear MPC	Nonlinear Model Predictive Control
LQR	Linear Quadratic Regulator
QP	Quadratic Programming